

The Science and Strategy for a Long-Baseline Neutrino Experiment Near Detector

DRAFT DRAFT DRAFT

M. Bishai, M.V. Diwan, Z. Isvan, E. Worcester
Physics Department, Brookhaven National Laboratory, Upton, NY

M. Bass, D. Cherdack, R.J. Wilson
Colorado State University, Fort Collins, CO

G.P. Zeller
Fermi National Accelerator Laboratory, Batavia, IL

L. Whitehead
University of Houston, Houston, TX

C. Mauger
Los Alamos National Laboratory, Los Alamos, NM

B. Mercurio, S.R. Mishra, R. Petti, X. Tian
University of South Carolina, Columbia, SC

(Dated: August 5, 2012)

Abstract

The defining characteristic for the Long-Baseline Neutrino Experiment (LBNE) is the length of the neutrino baseline, which must be sufficiently long to allow comprehensive and redundant measurements of the 3-generation neutrino oscillation model. All other issues: the depth of the detector, the type of detector, the scope and strategy of the near detector, although important, do not define the nature of the project since they can be enhanced or changed later. This realization and the prospects for the long term program of neutrino science has resulted in a preference for the option in which a far detector is sited at the Homestake site, 1300 km from FNAL, and a new beamline with the ability to handle power levels of 2 MW or above is constructed.

The financial constraints imposed on the LBNE project do not allow construction of a full near detector complex in the preferred or any of the other scenarios. The near detector could be constructed if resources other than the DOE HEP come into play. In this note, we examine strategies to maintain the initial scientific performance without a full near detector complex. Although detailed evaluation must await full simulations, it is our judgment based on previous experience that the options presented in this paper will be adequate for the initial period of LBNE running because of the choice of a liquid argon TPC for the far detector because of its extremely high performance in particle identification. Nevertheless, a full near detector complex is highly desirable in the long term, and is needed to achieve the full scientific agenda of LBNE.

I. OVERVIEW AND PURPOSE

With the discovery of non-zero θ_{13} , the next generation of long-baseline neutrino experiments offer the possibility of obtaining a statistically robust spectrum of muon and electron neutrinos and anti-neutrinos with large oscillation effects. Such measurements are scientifically well-motivated and well-appreciated as a unique capability in the U.S. Such long-baseline neutrino physics should remain a key objective in any phasing or reconfiguration plan that aims for U.S. leadership at the Intensity Frontier.

In long-baseline neutrino oscillation experiments, one searches for alterations in the composition of a neutrino beam as it propagates from its source to a Far Detector (FD) hundreds of kilometers away. The search broadly comprises three distinct but overlapping tasks. First, one must characterize the instrumental response of the FD to a neutrino interaction. This includes having detailed knowledge of final state particle multiplicity and kinematics - quantities that will be used to infer the incoming neutrino energy. Second, one must thoroughly characterize the beam at the source to properly account for potential differences in the beam between the source and FD. Third, in order to cleanly detect the oscillation signal and any accompanying neutrino/antineutrino differences, one must determine the prevalence and provenance of background events in both neutrino and antineutrino running.

The LBNE collaboration put forth a proposal for a 34 kt liquid argon (LAr) detector sited underground at the Homestake mine in South Dakota (~ 1300 km from Fermilab) and a smaller LAr TPC in conjunction with a very high resolution tracker as its ND. Budget constraints have since induced LBNE to proceed in phases. Three possible options for phase-I of LBNE were identified by the LBNE Reconfiguration Steering Committee:

1. 10 kt LAr TPC on the surface at Homestake (1300 km) and a new neutrino beam
2. 15 kt LAr TPC underground at Soudan (735 km) using the existing on-axis NuMI beam
3. 30 kt LAr TPC on the surface at Ash River (810 km) using the off-axis NuMI beam

The preferred option, recommended by the project and the LBNE Reconfiguration Steering Committee, calls for (1) a 10 kt LAr TPC on the surface at Homestake and a new neutrino beam. This choice makes certain that the truly unique aspect of the Long Baseline Neutrino Experiment experiment which is the 1300 km baseline is obtained in the first phase. This choice also allows a truly capable optimized broad band neutrino beam with future high power capability. If well executed the first phase offers a chance to discover the neutrino mass hierarchy (MH) and to detect CP violation in the neutrino sector. Nevertheless, the preferred choice abridges two important features of the LBNE science program, the underground physics and a rich ND program. The current document therefore examines various strategies for beam-related neutrino oscillation measurements in phase-I which aims to be consistent with budgetary constraints while providing sufficient systematic precision in characterizing the neutrino source and backgrounds for the MH and CP measurements. Note that this strategy and its associated costs can be different for the NuMI vs. Homestake options, as a near hall and some detector systems exist for the NuMI options.

In this, note we first describe the analysis issues in a long-baseline experiment. We then calculate the signal and background event rate expected for the Homestake and NuMI options. A brief review of previous experimental experience is followed by a number of possible options for LBNE for the initial phase of running. The options considered take into account the financial constraints that have been discussed in the FNAL Reconfiguration Steering Committee for phase I.

II. SYSTEMATIC PRECISION IN PHASE-I

Figures 1–3 show the expected spectrum of ν_e charged current (CC) events in a 34 kT FD at the Homestake and NuMI sites, in both neutrino and antineutrino modes for normal and inverted

mass hierarchies. Corresponding event rates are available in the appendix. The three dominant beam-induced backgrounds are from (a) neutral-current (NC) events, where a π^0 produced in the hadronic shower mimics a signal-like ('prompt') electron shower, (b) ν_μ CC interactions, where the outgoing muon is mistaken as an electron, and (c) intrinsic, irreducible beam ν_e events. All three backgrounds contribute approximately equally in the relevant energy range (0.5-8 GeV) although the NC background dominates at lower energies and the intrinsic ν_e background is fractionally a bit larger for Ash River than for the other options. The complete LBNE proposal stipulated a systematic error of 1% on ν_e signal expectation and 5% on the backgrounds, justified by ND studies. In Phase-I, however, the large reduction in the FD mass will cause the statistical error to dominate over the assumed systematic error in the ν_e appearance analysis for the first few years of running. Figure 4 shows how the statistical uncertainty on the appearance signal in both neutrino and antineutrino modes evolves in time. With the assumed (reduced) detector masses, the appearance measurements will be at the level of a 5-6% (8-10%) statistical error in 5 years of neutrino (antineutrino) running. Although the statistical precision for Phase-I will be less demanding it is important that (a) we can reliably estimate the systematic uncertainties without a full near detector complex and (b) we can estimate the overall background level and energy-dependence in a LAr TPC. The studies so far have relied on hand scans of simulated data to evaluate background expectations. The evaluations so far do not take into account spectral distortions or energy dependence.

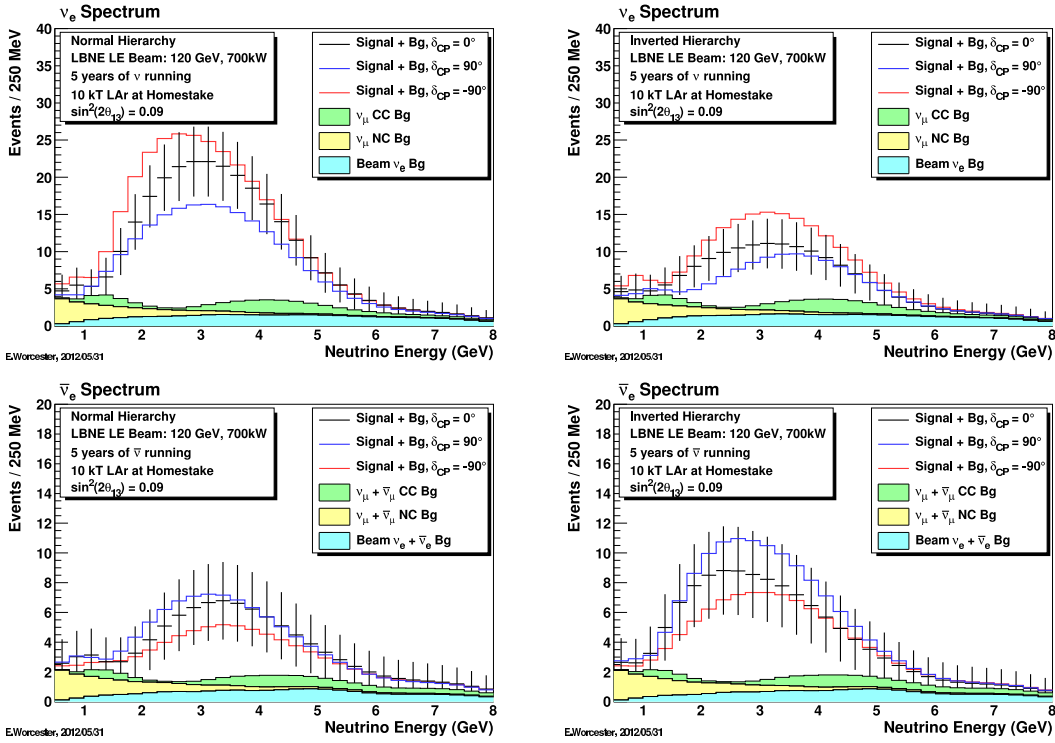


FIG. 1: Expected spectrum of ν_e events in 5 years of neutrino (top) and antineutrino (bottom) running for both the normal (top) and inverted (bottom) mass hierarchies for the Homestake option. The backgrounds induced by NC, ν_μ CC, and intrinsic ν_e are also shown. Plots are from E. Worcester (BNL).

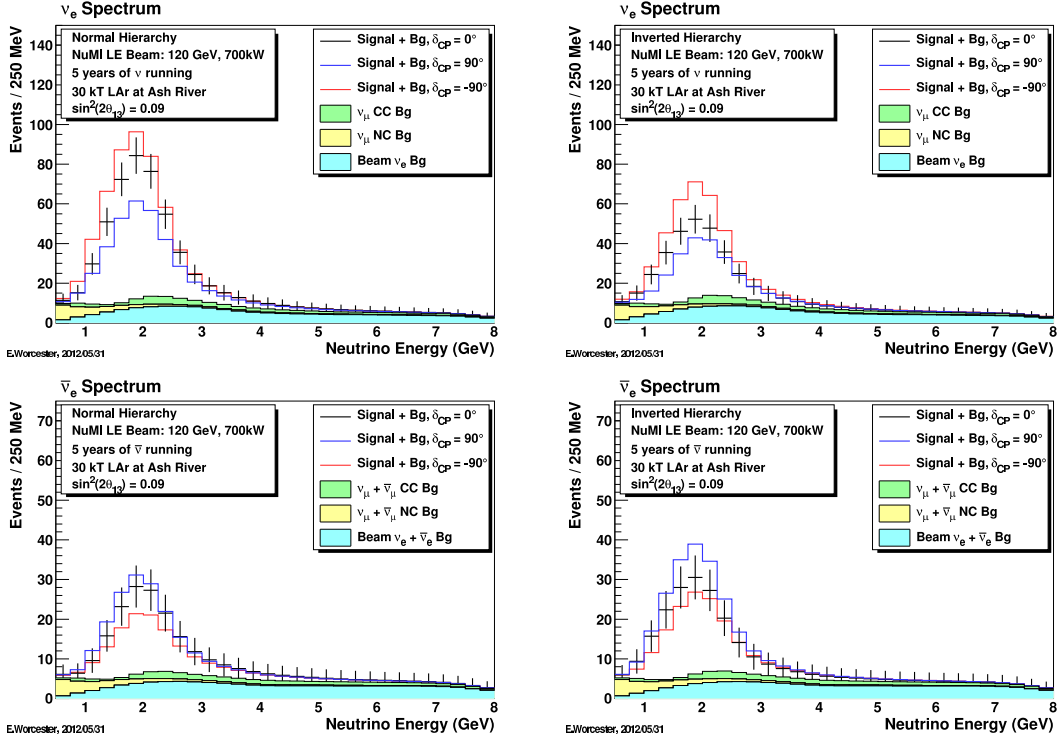


FIG. 2: Same as Figure 1 except for the Ash River option.

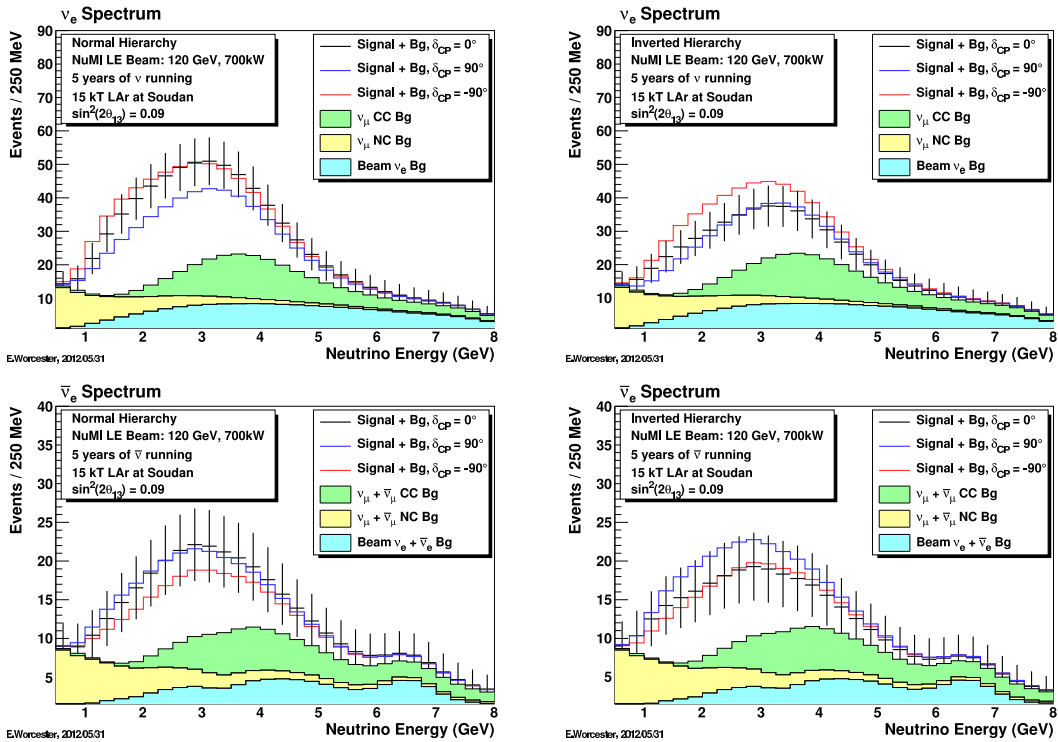


FIG. 3: Same as Figure 1 except for the Soudan option.

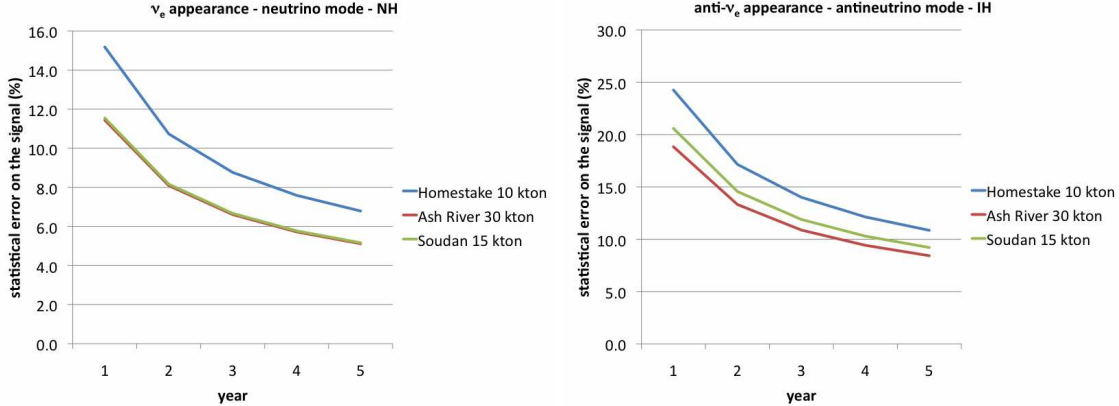


FIG. 4: Evolution of the statistical error on the appearance signals in time for both neutrino (left) and antineutrino (right) running. The highest statistics case is plotted in each case, meaning the normal mass hierarchy for neutrinos and the inverted mass hierarchy for antineutrinos. Signal rates are for $\sin^2 2\theta_{13} = 0.09$ and $\delta_{CP} = 0$ (see Appendix).

Given current background estimates, Figure 5 shows the effect of increasing the uncertainty on the signal and background normalization uncertainties for the mass-hierarchy and CP violation measurements in LBNE. These are the results from a GLOBES-based study where only the normalization on the signal and background are varied, assuming their energy spectrum is known. For Phase-I, the exacerbation of the normalization uncertainties from 5% to 15% for backgrounds and from 1% to 5% for signal events is smaller than, for example, the full 34 kt FD where the statistical precision demands better systematic determination of both signal and background. Therefore, given the smaller FD masses, we can tolerate larger systematics in Phase-I for the highest priority goals of LBNE: parameters that govern the $\nu_\mu \rightarrow \nu_e$ conversions.

The situation is different for the disappearance measurements. There, the anticipated event rate is naturally much larger than for the appearance measurements and hence the statistical uncertainties are smaller. Figure 6 shows how the statistical uncertainty on the disappearance event rate evolves in time. With the assumed (reduced) detector masses, the disappearance measurements will be at the level of a 0.8-2.0% (1.1-2.8%) statistical error in 5 years of neutrino (antineutrino) running, depending on the baseline. Obviously, with the shorter baseline for Soudan, the overall statistics are much larger and hence the statistical errors are smallest in that case.

Although the statistics of the disappearance mode are higher, the nature of the signal and how it affects the measurements of Δm_{23}^2 and θ_{23} need to be carefully considered. For the Homestake baseline of 1300 km, the signal is a clear oscillatory pattern that can be measured regardless of the presence of a near detector (see Figure15). For the NuMI options the signal is a depletion of events without a large spectral distortion, and therefore has a larger dependence on the accuracy of the event rate prediction. For LBNE, the full analysis of the oscillatory pattern will need to be performed to understand how it depends on the systematic errors on the expectation.

For all of the Phase-I options, the increased statistics expected in the disappearance channel and the need to accurately measure distortions in the observed ν_μ and $\bar{\nu}_\mu$ spectra, increases the need for ND measurements.

Having established that the level of systematic uncertainty required in Phase-I of LBNE will be different for the appearance and disappearance measurements, the next section will summarize the level of precision that has been achieved in previous experiments that have conducted neutrino oscillation searches, and the techniques that have been used to achieve that precision.

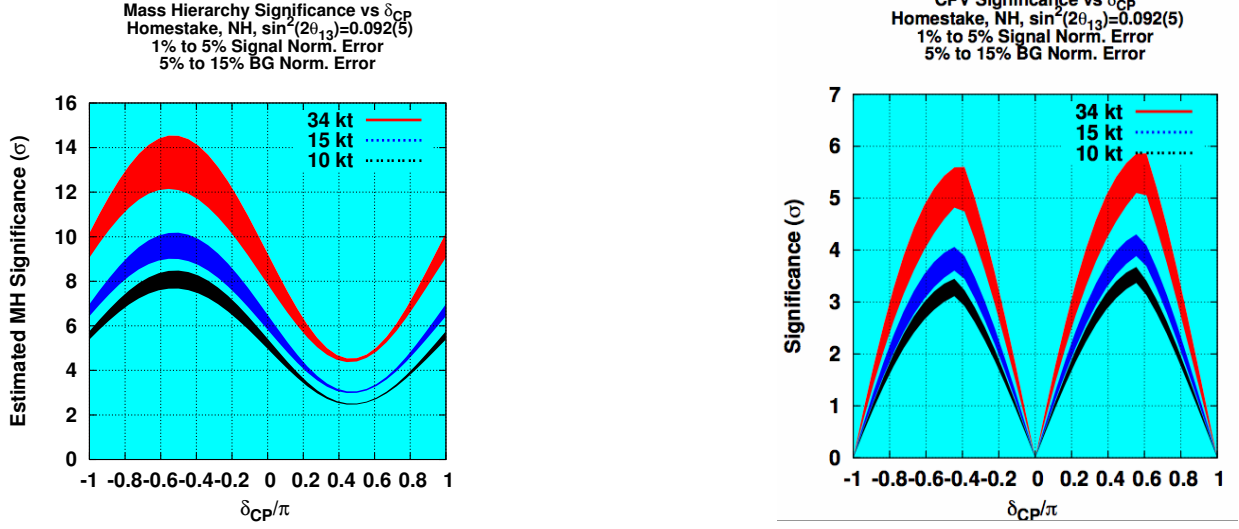


FIG. 5: Mass hierarchy (left) and CP violation (right) sensitivity for a range of assumed background and signal normalization errors for a 10, 15, and 30 kt far detector at Homestake. In this study, the shape of both the signal and background events are assumed to be known and only the normalization uncertainties are varied.

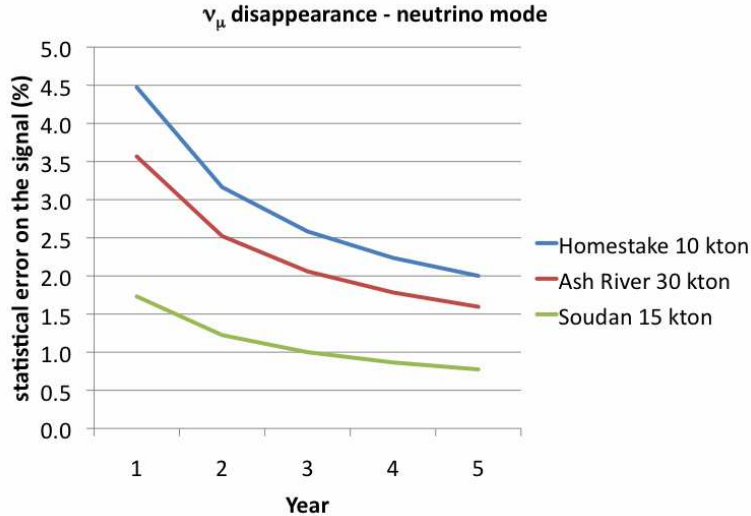


FIG. 6: Evolution of the statistical error on the disappearance signals in time for both neutrino (left) and antineutrino (right) running. Signal rates are for oscillated events assuming $\Delta m_{23}^2 = 2.3 \times 10^{-3} eV^2$ and $\sin^2 2\theta_{23} = 0.705$ (see Appendix).

III. PREVIOUS EXPERIMENTAL EXPERIENCE

Past searches for $\nu_{\mu} \rightarrow \nu_e$ oscillations at large Δm^2 (short-baseline) include E734, E776, K2K, MiniBooNE, MINOS, and NOMAD. With the exception of MINOS and K2K, these were all single-detector experiments with NC π^0 and intrinsic beam $\nu_e s$ as the dominant backgrounds. Table I

summarizes the overall systematic error in the $\nu_\mu \rightarrow \nu_e$ appearance search achieved by these experiments. With the exception of NOMAD, none of these experiments had a resolution better than what is expected from a LAr TPC. A brief synopsis of systematic errors achieved by these experiments is given below. The description does not exactly correspond to the table because of the ambiguities in interpreting the numbers from each publication. The table also does not account for the spectral information used in those experiments, nevertheless it allows an approximate idea of the previous experience. The two experiments based on the SuperKamiokande far detector, K2K and T2K, are omitted from the table because of recent changing analysis of T2K, summarized in the sections devoted to those experiments.

Experiment	NC/CC (π^0) Events	Beam- ν_e Events	Syst.Error	Comment
E734	235	418	20%	No ND
E776(89)(NBB)	10	9	20%	No ND
E776 (WBB)	95	40	14%	No ND
MiniBooNE (>450MeV)	140	250	9%	No ND
MINOS	44	5	5.6%	ND-FD
NOMAD	<300	5500	< 5%	No ND

TABLE I: *Summary of achieved systematic error performance in some past $\nu_\mu \rightarrow \nu_e$ oscillation experiments. Table is from [2]. These numbers were extracted from publications to the best of our ability and do not correspond exactly to the description in the text.*

A. E734

The experiment BNL-E734 could be considered a model of a high granularity, large, surface detector that operated successfully and produced a number of results in neutrino physics in the 1980's. The publications have been collected in a single volume for convenience [4]. Here, we summarize the analysis that led to a limit on the appearance of electron neutrinos from muon neutrinos.

The E734 detector was specifically designed to measure electro-magnetic showers, in particular the reactions $\nu + e \rightarrow \nu + e$ which are rare events. The detector consisted of 112 planes of liquid scintillator each 8 cm thick and $4\text{ m} \times 4\text{ m}$, and 224 planes of proportional drift tubes ($4.2\text{ m} \times 4.2\text{ m} \times 3.8\text{ cm}$). The fine segmentation (1792 scintillator cells, and 12096 proportional drift tubes) allowed determination of event topology, identification of EM showers, and substantial discrimination through dE/dx of electrons, photons, pions, and protons. In comparison, the capability of a liquid argon tracking chamber should be even better than E734.

The analysis strategy for E734 relied on first extracting the electron neutrino signal using the good particle identification capability of the detector. After signal extraction, a ratio of electron and muon neutrino quasielastic interactions was formed and compared to a Monte Carlo calculation. The ratio technique allowed cancellation of systematic errors due to cross section uncertainties.

An initial sample of 653 showering events was selected by software and eyescan. Events were first examined for evidence of the $\pi \rightarrow \mu \rightarrow e$ decay and eliminated bin by bin. A second set of showering events was selected with a large upstream energy deposit which tagged the event as a photon. The second set was normalized in the low energy (<0.9GeV) region and subtracted from the first set. The final signal distribution of electron neutrino events contained 418 events

in the energy region 0.9 – 5.1 GeV. After extraction of muon neutrino data, a ratio was formed of the measured electron neutrino flux and the muon neutrino flux. There were two significant systematic errors: (1) the muon and electron data sets were over somewhat different Q^2 regions and therefore had differing acceptance factors, and (2) the modeling of neutrino flux depended on uncertainty in the K/π ratio which was poorly known at the time of the analysis. The two systematics combined were estimated to be about 20%. One measure of the performance of the experiment is the mixing angle limit at large Δm^2 . This mixing angle limit depends on the electron neutrino background level ($< 1\%$ in E734), and the statistical and systematic errors in the experiment. E734 achieved a mixing angle limit of 3×10^{-3} at 90% C.L. for large Δm^2 .

The E734 technique of background tagging and reduction can be easily used for a LAr-based LBNE experiment. The ratio technique will need to be adapted because of the large disappearance oscillation expected in the muon mode. Since the K/π ratio is now known much better from external measurements, the E734 style of systematic error should be reducible down to $< 14\%$.

B. E776

BNL-E776 was an experiment specifically designed to search for $\nu_\mu \rightarrow \nu_e$ oscillations over a baseline of ~ 1 km using a neutrino beam from the Brookhaven AGS. The detector took data in both narrow-band and wide-band beams. The results are in two papers [5, 6]. The results from the wide-band beam have higher statistics and better sensitivity. We will summarize the wide-band analysis here and draw some lessons for LBNE.

The E776 detector was 230 ton and composed of 90 planes of proportional drift tubes interleaved with 1 inch thick concrete absorber. Each plane of PDT with absorber corresponded to 0.3 radiation lengths and 0.08 interaction lengths. There was a magnetic muon spectrometer at the downstream end of the detector.

The data analysis proceeded by using pattern recognition software to select clusters of hits in the detector. These clusters were identified as muon or shower type. The shower type events were further examined to select electron type showering events with a dense well-collimated core and a clear evidence of gaps signaling energy loss due to the presence of photons in the shower. Since the detector was not completely live, as was the case with the E734 detector, there could be no cuts on vertex activities to identify backgrounds due to π^0 's. Therefore the E776 analysis relied on a calculation of the probability of misidentifying a π^0 event as an electron event. This calculation was, however, normalized by the data in which π^0 events were correctly identified. The systematic error on the π^0 background determination included the statistical error from the identified π^0 sample. This error was in the range of 30 to 40% for neutrino and antineutrino data across the energy range of a few hundred MeV to a few GeV. The systematic error on the background from electron neutrino contamination in the beam was estimated to be 11%.

The final sample of data for neutrino running was 136 events with expected background of $131 \pm 12(stat) \pm 20(bck\ stat) \pm 19(syst)$. Above 1 GeV there were 56 electron candidate events with expect background of $62 \pm 8(stat) \pm 5(bck\ stat) \pm 7(syst)$. For anti-neutrino running, the final sample was 47 events with expected background of $62 \pm 8(stat) \pm 13(bck\ stat) \pm 9(syst)$. Above 1 GeV, the antineutrino data had 19 events with expected background of $25 \pm 5(stat) \pm 3(bck\ stat) \pm 3(syst)$. As can be seen, the systematic error on the background estimate was obtained to be approximately in the 11 to 14 % range. The background estimate was assisted by using events that were identified to be π^0 events. This technique contributed a further error due to the statistics of the background sample (indicated as *bck stat*). Using this event sample and systematic errors, E776 achieved a mixing angle limit of 3×10^{-3} at 90% C.L. for large Δm^2 .

The contrast between the E776 analysis and the E734 analysis is very useful to study for LBNE using a liquid argon detector. E776 analysis was not able to utilize vertex activity to tag

background photons and had to rely on Monte Carlo simulations for the π^0 background estimate. The two analysis also differ greatly over the background estimate uncertainty for the electron neutrino contamination. This is most likely due to the increased understanding of the neutrino beam modeling in the E776 analysis.

C. K2K

K2K, the first modern era long-baseline experiment with a man-made neutrino beam, ran from 1999 until 2004 with a beam produced at KEK and detected in the Super-Kamiokande detector in Kamioka, 250km away. K2K extensively used a broad range of measurements made at the near-site for both rate and spectral monitoring and systematic uncertainty evaluation and reduction. K2K explored both muon neutrino disappearance and electron neutrino appearance in a muon neutrino beam. For both cases, quasi-elastic-like events were chosen for the analysis as these events in a water Cherenkov detector are easy to identify with good particle identification properties. For electron neutrino appearance, the largest background is due to single neutral pion production from neutral current interactions. This background and its uncertainty were estimated using the high-statistics data available in the near-site water Cherenkov detector. The signal expectation required an estimate of the un-oscillated muon neutrino energy spectrum. The spectrum was measured using the neutrino detectors at the near site. The K2K experimental statistics were low and the sensitivity was limited by the statistics of the experiment. A single electron type event was detected with a background expectation of 1.7 with a systematic error of $\sim 30\%$. A large fraction of the error was due to the π^0 rejection cut in the water Cherenkov detector.

D. MiniBooNE

MiniBooNE was designed to search for ν_μ to ν_e and $\bar{\nu}_\mu$ to $\bar{\nu}_e$ transitions across a relatively short distance (541 m) and hence was sensitive to neutrino oscillations at high Δm^2 . Neutrino events were detected in a 610 cm radius spherical tank filled with 800 tons of ultra-pure mineral oil (CH_2) and lined with 1280 8-inch photomultiplier tubes. A separate outer veto region instrumented with 280 photomultiplier tubes allowed charged particles entering the tank from outside or events that were not fully contained in the main tank to be excluded from the analysis. Using the registered pattern, charge, and timing of both Cherenkov and scintillation light recorded in the photomultiplier tubes, different event classes could be distinguished, thus allowing searches for both ν_e appearance and ν_μ disappearance.

For the $\nu_\mu \rightarrow \nu_e$ appearance searches, electron-like quasi-elastic events were selected and reconstructed. Quasi-elastic events were chosen because they are the dominant interaction in the MiniBooNE beam and because the incoming neutrino energy can be reconstructed solely from the outgoing electron kinematics. Fits for both ν_e and $\bar{\nu}_e$ appearance were conducted over neutrino energies ranging from 200 MeV up to 3 GeV [8]. In the final neutrino mode analysis, an excess of 952 events was observed over the energy range from 200-1250 MeV in 6.46×10^{20} POT over a predicted background of 790.0 ± 28.1 (stat) ± 38.7 (syst) events [9]. In antineutrino mode, 478 events were observed over a background of 399.6 ± 20.0 (stat) ± 20.3 (syst) events in 11.27×10^{20} POT [9]. Backgrounds in MiniBooNE were dominated by NC, intrinsic ν_e , and ν_μ CC events as well as a small source stemming from neutrino interactions originating outside the detector. In the energy range of interest for oscillations (200-1250 MeV), roughly 43% of the backgrounds to the ν_e sample were predicted to be NC (both π^0 and single γ production), 43% beam ν_e , 10% ν_μ CC, and 4% from neutrino interactions occurring outside the detector volume. Given the short-baseline and the small distortions expected in the ν_μ spectrum across these distances, the backgrounds could be directly constrained from measurements of ν_μ interactions in the MiniBooNE detector itself (i.e., without a near detector). The NC π^0 production rate was constrained to $\sim 5\%$ based on the measurement of cleanly reconstructed NC π^0 events in the detector. The final uncertainty on NC

backgrounds was thus dominated by $\sim 20\%$ uncertainties in the mis-identification rate of NC events in the MiniBooNE detector, entirely stemming from detector uncertainties. The uncertainty in ν_e backgrounds resulting from muon decays in the beam were heavily constrained (to the few-% level) by the measurement of ν_μ events from pion decays, while ν_e from kaon decays were constrained (to $\sim 25\%$) by high energy ν_μ events both in the MiniBooNE and SciBooNE detectors. Backgrounds stemming from interactions of neutrinos outside the detector were constrained to $\sim 15\%$ using the measured radial and z distributions of neutrino events reconstructing at large radii. In the end, the total integrated background in MiniBooNE was determined to 6% (7%) in neutrino (antineutrino) mode; however, this uncertainty was quite energy dependent. Such uncertainties were possible without a dedicated near detector because of the high statistics samples of undistorted ν_μ (and $\bar{\nu}_\mu$) events available in the MiniBooNE detector.

E. MINOS

MINOS is a long-baseline neutrino oscillation experiment that measures the oscillations of muon neutrinos in the NuMI neutrino beam-line. The near (0.98 kT) and far detectors (5.4 kT) consist of alternating layers of steel plates and scintillator strips. Both the near and far detectors have identical segmentation of 1 inch (1.44 radiation length) steel and 1 cm thick plastic scintillator. Transversely the scintillator is in strips of 4.1 cm width, corresponding to Moliere radius of 3.7 for electromagnetic showers. The scintillator is read by wavelength shifting fibers into multi-anode PMTs. The scintillator strips range in length from a maximum of 8 meters in the far detector down to ~ 1 m in the near detector. The NuMI facility can produce neutrino or antineutrino beams, and the neutrino energy spectrum can be tuned by changing the position of the target. The beam has operated primarily in a low-energy neutrino beam configuration over the lifetime of MINOS.

Though the MINOS detectors were not optimized for detection of electron neutrinos, the MINOS electron neutrino appearance search achieved excellent sensitivity to θ_{13} . Early results [12, 13] were based on a rate-only measurement, where the signal selection was done based on an artificial neural network that used variables related to event topology as inputs. More recent results [14, 15] employ a selection algorithm that labels input events as signal-like or background-like based on their similarity to events in a library of simulated signal and background events and use a shape fit in both energy and the selection variable. The final analysis will also include data from the antineutrino beam mode [15].

The signature of a ν_e charged current (CC) interaction in MINOS is the energy deposition from the electron in a relatively narrow and short region, overlapping with the activity from the hadronic recoil system. The main background is due to neutral current (NC) interactions, where the hadronic recoil system produces a similar topology, especially if a π^0 is present. Other background contributions come from the intrinsic electron neutrino contamination in the beam, low-energy ν_μ CC interactions with a short muon track, and ν_τ CC interactions (from $\nu_\mu \rightarrow \nu_\tau$ oscillations). For an exposure of 8.2×10^{20} POT, MINOS expects 49 far detector (FD) background events in the signal region, of which 34 are NC, 7 are ν_μ CC, 6 are beam ν_e CC, and 2 are ν_τ CC [14].

Electron neutrino appearance in MINOS is observed as an excess of ν_e CC events at the FD over the background predicted based on ND data. To make the background prediction, the selected ND data must first be broken down into the different types of background interactions, as the extrapolation of each component to the FD is affected differently by oscillations and beamline geometry. The signal selection is applied to ND data taken in several beam configurations with different energy spectra. Using these data sets, a linear system of equations can be constructed and solved for the relative contributions of the different background types in the standard low-energy beam mode. Once the backgrounds have been separated in the ND data, ratios of FD to ND rates from simulation (in bins of energy and the selection variable) are used to translate the ND data rates to FD background predictions.

The systematic uncertainties on the far to near ratios are relatively small, as uncertainties due to neutrino flux and interaction modeling largely cancel. The total systematic uncertainty on the predicted number of background events in the signal region is 5.4%, with the largest contribution coming from the uncertainty in the relative far/near energy scale[14]. For comparison, the systematic uncertainty on the FD background from simulation alone (as opposed to the far to near ratio) is roughly 30%, dominated by hadronic shower modeling uncertainties.

It is instructive to compare the MINOS experience with E776 and E734. The MINOS detector has much less granularity and therefore has much lower ability to separate background samples in the far detector. The MINOS near detector is used to measure the background and largely compensates for the poor event recognition ability of the far detector. For example, with much better pattern recognition in a liquid argon TPC, the shower modeling could be tuned on a subset of events that are selected to be background resulting in smaller modeling uncertainties.

F. NOMAD

NOMAD was a low-density ($\rho \approx 0.1 \text{ gm/cm}^3$) fine-grain tracker. It was designed to search for τ -appearance in $\nu_\mu \rightarrow \nu_\tau$ oscillations. Charged particles were tracked by light drift chambers; the electron-ID was achieved by TRD, preshower, and ECAL subdetectors. The tracker and preshower-ECAL were embedded in a dipole B-field (0.4 T). Outside and downstream of the magnet were muon-detectors and an HCAL. The fine-grain tracker originally envisioned for LBNE ND complex, HIRESMNU [?], is built on the NOMAD experience. It improves upon NOMAD in electron-ID, charged particle tracking, and provides 4π calorimetric and muon coverage. Because NOMAD could distinguish e^- from e^+ and reconstruct the missing- P_T vector on an event-by-event basis, the π^0 -induced background could be kept at a very low level ($\sim 5\%$ in the $\nu_\mu \rightarrow \nu_e$ search). As shown in Table I the high resolution, excellent π^0 rejection, and high statistics in the muon mode allowed NOMAD to achieve extremely good systematic error performance, $< 5\%$, on the backgrounds. As a result NOMAD achieved a mixing angle limit of 1.4×10^{-3} for large Δm^2 at 90% C.L.

G. T2K

The primary goal of the T2K experiment [16] is to measure θ_{13} to high precision using a high purity off-axis narrow-band muon-neutrino beam with a peak energy of approximately 0.6 GeV. The beam is produced at the Tokai accelerator complex [18], and the SuperKamiokande (SK) detector [17] located 295 km downstream of the target in the Kamioka mine. The ultimate precision of the measurement relies on the reduction of systematic uncertainties through constraints provided by a near detector.

The T2K Near Detector (ND280), located 280 m downstream of the target, is comprised of several sub-detectors in a magnetic field. The upstream portion, called the Pi-zero Detector (P0D), was designed to detect neutral pions produced in hadronic showers, as well as the electron neutrino component of the beam. These events comprise a main source of background for the electron appearance measurements at the heart of the T2K experimental program. Surrounding the P0D is the a calorimeter (Ecal), which is responsible for detecting any electromagnetic energy escaping the P0D, thus ensuring full containment of electromagnetic (EM) energy originating in the P0D. Downstream of the P0D is the Tracker. The Tracker is composed of three time projection chambers (TPCs) interleaved with fine grained scintillator detectors (FGDs). The Tracker is designed to measure the muon energy spectrum, which is required to constrain the muon neutrino flux accurately.

The SuperKamiokande detector is a water Cherenkov detector with a fiducial mass of 22 kt. The target material of the near and far detectors differ, thus the near detector must constrain

the flux and cross sections independently, rather than directly using the ND280 event rates to predict the SK unoscillated spectrum. In order to measure the cross sections on water, the POD was designed as a water target. When planar water bags, interleaved with the active scintillator layers, are filled the primary inactive detector material is water. The water bags can be emptied, and water only cross sections can be measured by examining the difference in event rates between the "water in" and the "water out" modes of operation.

In this early stage of operation ($\text{few} \times 10^{20}$ POT), statistical uncertainties dominate the T2K electron neutrino appearance measurement and the systematic constraints from ND280 have little effect. The main contribution thus far has been to constrain the flux models with muon data in the tracker. Nonetheless, much effort has gone into a simultaneous fit of flux and cross section parameters using ND280 analyses, along with results from other experiments (such as MiniBooNE, SciBooNE, etc), to help constrain SK event rate prediction used in the oscillation analyses. Using this procedure, the total systematic uncertainty from all sources (beam flux, neutrino interaction uncertainties - including final state interactions, and far detector uncertainties) was reduced from roughly 20% in the preliminary results presented in 2011, to around 11% presented by T2K at the Neutrino 2012 conference [19]. As exposure increases, and statistical uncertainties are reduced, the machinery for constraining the fluxes and cross sections on water will determine the overall precision on the T2K oscillation searches. Assuming the current central value for θ_{13} , by 2015 the number of events in the analysis sample (signal + background) is expected to increase from 9.07 ($6.61 + 2.47$) to approximately 64 ($47 + 17$) with a systematic uncertainty of less than 10%.

In addition to contributing the oscillation physics goals of T2K, ND280 is also able to provide a myriad of cross section analyses. The high statistics and excellent spatial resolution of the detector allow for the measurement of many cross sections and cross section parameters in each sub-detector. Short baseline (sterile neutrino) oscillation searches, and tests for other exotic (beyond the standard model) physics are also enabled by the near detector.

IV. ROLE OF THE NEAR DETECTOR

Measurements using the instrumentation at the near site includes hadron and muons counters in the beam as well as the near neutrino detector. These provide a variety of constraints on the systematic uncertainties of long-baseline experiments. Here, we discuss two issues, the role of the near neutrino measurements in constraints throughout the running period and the role in constraining the neutrino energy spectrum.

A. Needs Throughout the Run

The K2K experiment monitored the neutrino beam stability directly by high-statistics measurements at the near site. Both the rate and spectrum were carefully measured as shown in Figure 7. The beam profile was obtained from the vertex distribution of charged current muon neutrino interactions. By measuring the muon momenta and direction with respect to the neutrino beam, K2K was able to demonstrate control of the neutrino energy spectrum to 2 – 4% depending on the bin. A similar exercise was also performed for the MINOS experiment. It was highly successful and resulted in a new understanding of the degradation of the NuMI target system. LBNE will employ a high-intensity proton beam and thus need to make careful measurements to constrain any changes in the neutrino beam throughout the run.

B. Spectral Information

There are two significant ways in which near neutrino measurements contribute to an understanding of the spectral information at the far site. First, they provide a constraint on the far-near

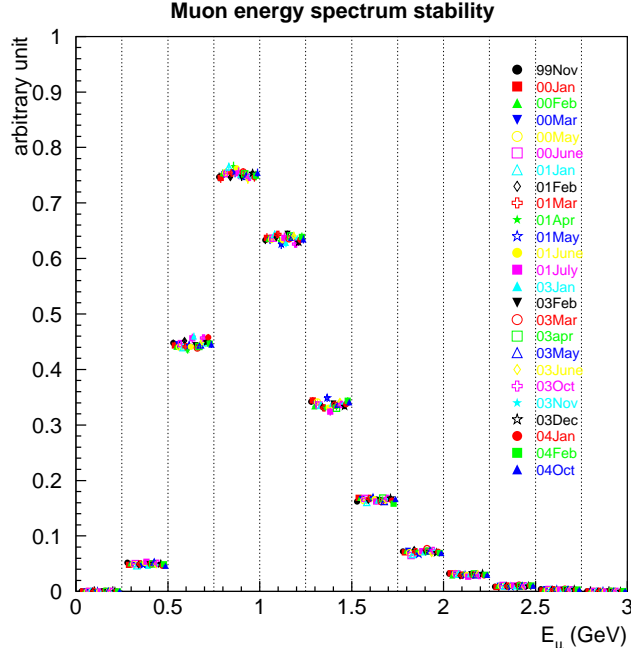


FIG. 7: Stability of the muon energy distribution as measured in the K2K muon range detector from [20].

ratio that is used to predict the signal and background in the far detector. Second, they provide high-statistics and high-precision data with which neutrino interaction simulation programs can be checked and modified.

In general, the non-oscillated neutrino spectra at the near and far site are different due to parallax effects. Long-baseline experiments account for this by constructing a far-to-near ratio. The initial ratio is constructed using a beam MC (using detailed geometrical information of the beam-line) that is validated with high-statistics hadron production data usually taken in external beam-lines. The ratio is then validated with measurements of the secondary hadrons or tertiary muons in the beam-line where the neutrinos are created. The neutrino spectrum is then measured at the near site. With this information, predictions for the signal and background at the far site are possible with high precision.

LBNE will employ a large liquid argon TPC at the far site and will attain sufficient statistics by using the inclusive charged current cross-section. It is important for LBNE to understand the event signatures that will be produced by neutrinos through approximately 5 GeV. The event signatures will have both intrinsic physics effects as well as detector instrumental effects. MicroBooNE will provide information at lower energies, but MicroBooNE measurements must be extrapolated to higher energies unless there is another experiment that will measure neutrino interactions on the argon nucleus through 5 GeV. The bulk of the interactions in the energy regime important for oscillation physics is the resonance regime. It is below the deep-inelastic scattering regime and well above the low-energy nuclear reaction regime where the cross-sections are reasonably-well understood. Neutrino-nucleus cross-sections have large uncertainties in the resonance regime, but the final-state interactions of the outgoing hadrons are less constrained.

In an oscillation analysis, effectively, a probability distribution for the true neutrino energy and flavor is constructed using reconstructed quantities. Final-state interactions play a large role in determining how well the true neutrino energy is determined in each event. An additional difficulty arises when one considers the neutrino beam is not the CP mirror of the anti-neutrino beam. Also, since nuclei consist of matter, an additional CP asymmetry is introduced in the interactions. Detailed neutrino interaction measurements at the near site allow us to constrain

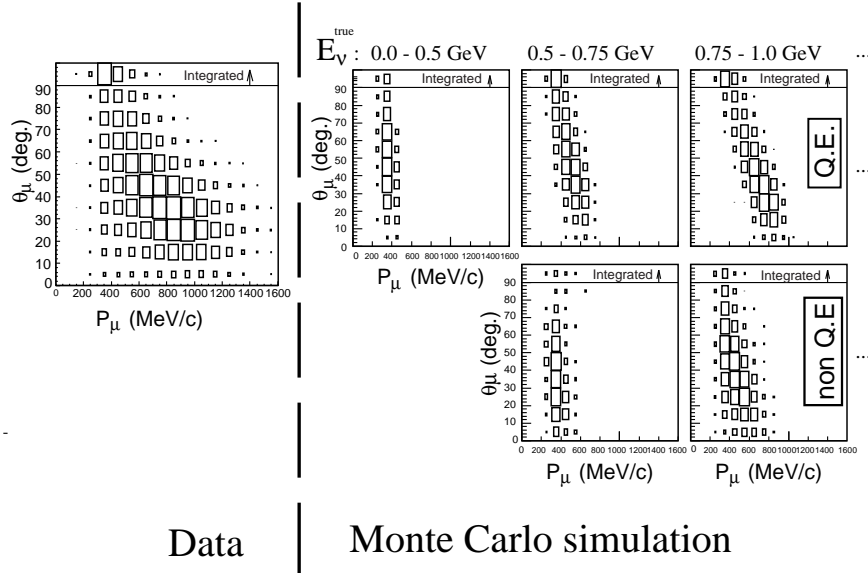


FIG. 8: The left plot shows the K2K data in the near water Cherenkov detector while the right panel shows the simulation of data from three sets of neutrino energy. The upper portion of the right panel shows events from true quasi-elastic interactions, while the lower portion contains events reconstructed as quasi-elastic events but which come from non-quasi-elastic interactions. Plot is reproduced from [20].

the uncertainties associated with the above challenges.

K2K used its near detector to understand the contribution of non-quasi-elastic events in the quasi-elastic sample at the far site as shown in Figure 8. In addition, using a variety of near-detector event samples, K2K scaled various processes in its event generator to reduce the uncertainty associated with the prediction at the far site.

In LBNE, the detailed measurements on the argon nucleus at the near site will play an important role in the long-baseline analysis. For measurements that are similar to counting experiments, the spectral issues play a role in determining which events are in or out of the count. They also play a role in understanding how many signal events one should have in one case or another (e.g., the neutrino mass hierarchy measurement). While it is plausible these measurement could be carried out in the absence of near neutrino measurements, it has not yet been demonstrated. For measurements that more strongly depend on neutrino spectral information, detailed near-site neutrino measurements on the same target nucleus are highly desirable.

V. OPTIONS FOR LBNE

Options for possible near detector measurements are different for the various reconfiguration choices due to the availability of existing near site resources in some of the cases. Table II summarizes existing (or soon to be existing) near site resources. Although the NuMI options have a big advantage in having near site halls, none of the options satisfy the requirement of having an essentially identical detector with the same nuclear target for a robust near site measurement. In addition to the resources in the table, it is possible to place detectors on the surface above the beam dump in each case. Such a near surface detector will detect off-axis neutrinos from the beam-line.

configuration	existing ND hall	existing near detectors
Homestake 10 kton	N/A	N/A
Soudan 15 kton	NuMI on-axis near hall	MINER ν A, MINOS ND
Ash River 30 kton	NO ν A off-axis near hall	NO ν A ND

TABLE II: *Existing near site infrastructure for the various options.*

A. Signal and Background Evaluation with Far Detector Data Alone

As pointed out previously, one of the advantages of the LAR TPC far detector is the high resolution and superb particle identification. This performance of the detector can be used to subdivide the far detector data set into many distinct samples that can be studied. As in the previous single-detector $\nu_\mu \rightarrow \nu_e$ experiments, the FD itself will provide control data samples which will help further constrain π^0 backgrounds and intrinsic ν_e which, after all, come from muon-decays (which in turn come from pions which are the dominant source of ν_μ CC or $\bar{\nu}_\mu$ CC), and kaon-decays. The detailed analysis of event topologies has started with eye-scans, but will require significant effort over the next few years. The detailed distributions for several topologies can be fit using the Monte Carlo calculations which can place constraints on the neutrino interaction models on Argon. This method will be carried out regardless of the near detector, and of course a near detector with much higher statistics will be important for further consistency checks.

Finally the atmospheric neutrino-oscillation parameters ($\nu_2 \rightarrow \nu_3$) will have been well measured by the NO ν A and T2K experiments. Using the precisely known θ_{23} and Δm_{23}^2 , and using the FD ν_μ and $\bar{\nu}_\mu$ CC data, one can extract further constraints on the neutrino flux. This technique is obviously not satisfactory for making a self-consistent comprehensive measurement of the neutrino properties. However, in Phase-I of the experiment this technique could provide adequate understanding of the expected spectrum to obtain the first results on CP and mass ordering.

B. Tertiary Muon Measurements

The LBNE neutrino beam is produced by impinging the primary proton beam onto a target embedded in a pulsed magnetic horn. The secondary particles produced, hadrons (mostly charged pions), are focused down a decay region. Charged pions decay mostly into neutrinos - producing the neutrino beam - and muons. Most of these tertiary muons penetrate the absorber and can be measured in the space just downstream of the absorber.

The standard LBNE Near Detector Complex includes measurements of the spectrum at the absorber hall and measurements of the neutrino spectrum a few hundred meters downstream in an underground hall built on-axis with respect to the neutrino beam. Phase I of LBNE currently includes neither the detectors nor the hall for neutrino measurements.

The effort associated with measuring the neutrino fluxes and spectra at the absorber hall include the planning of measurements of hadron production in external beam-lines and measuring the tertiary muons that penetrate the absorber. Figure 9 shows the detector systems that have been designed to measure the tertiary muon spectrum after the absorber in LBNE.

Previous experience with using muon measurements from a beam-line is documented in a thesis by Loiacono[21]. The measurements from the MINOS muon ionization monitors were used to constrain the neutrino flux using a detailed Monte Carlo calculation. The measurement required the ability to change the target/horn tune of the beamline to obtain spectra of different muon energies (or penetration). The LBNE system is designed to overcome some of the challenges of the MINOS system: the muon monitors are Michel decay detectors that should be more robust against pile up issues in ionization monitors, and secondly the LBNE monitors are spaced closer at lower muon energies that are more relevant for the neutrino spectrum.

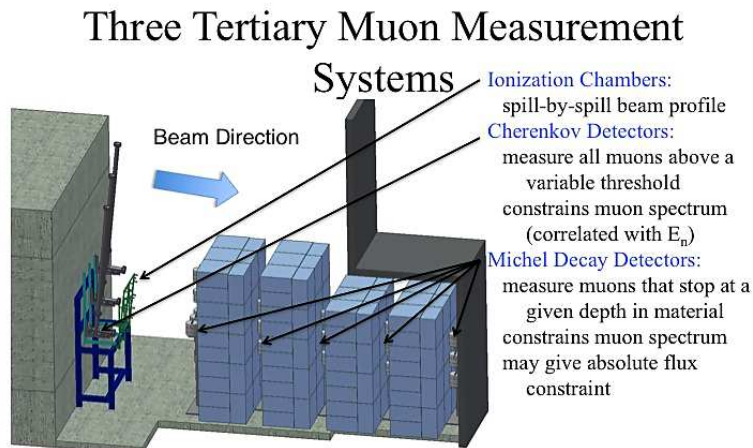


FIG. 9: Proposed tertiary muons systems for LBNE.

C. Reduced Cost Option: Near Detector in a Shaft

While the full-design of the LBNE near detector has the capability required for all phases of the experiment, there are options that would be lower cost with reduced capabilities. The standard LBNE near neutrino detector requires an underground hall with two shafts. One option to reduce cost but still make on-axis neutrino measurements at the near site is to construct only one of the shafts. A detector would then be commissioned on the surface and lowered into the shaft to be positioned for on-axis measurements. The standard LBNE shaft is twenty-two feet in diameter. Figure 10 shows a design for a detector that can be employed to measure on-axis neutrino interactions with argon, the nuclear target of the far site.

The detector consists of steel and scintillator planes with a toroidal field and argon gas targets. There are three regions to the detector: upstream, mid-region and downstream. One module in the upstream and downstream region consists of a plane of one-inch thick steel and two planes of scintillator bars. The planes of scintillator are oriented such that the longitudinal direction of the bars in one plane are perpendicular to those in the other. The upstream consists of twenty modules giving three nuclear interaction lengths of instrumented steel to reject entering background. The downstream region consists of forty modules and is employed to measure charged particles (e.g. muons) from the central interaction region. The central region consists of 2.75 inch (OD) stainless steel tubes with eighth-inch thickness. These can be filled with 100 atmospheres of argon gas. With this thickness, positional selection criteria are used to define a fiducial volume where neutrinos interactions on argon outnumber those on steel by a factor of ten. The planes of tubes are alternated with two planes of solid scintillator bars similar to the modules in the upstream and downstream regions of the detector. Magnet coils penetrate the detector to generate a toroidal magnet field (similar to MINOS).

This configuration measures the aggregate of the intrinsic electron neutrinos and anti-neutrinos on argon as a function of reconstructed neutrino energy. Also, it measures muon neutrinos and muon anti-neutrinos separately as a function of reconstructed (anti-)neutrino energy by the sign-selection capability from the toroidal field. Many of the gamma-rays from neutral pions will convert in the central region. This configuration therefore measures the two primary backgrounds to electron (anti)neutrino appearance - neutral current events and intrinsic electron (anti)neutrinos;

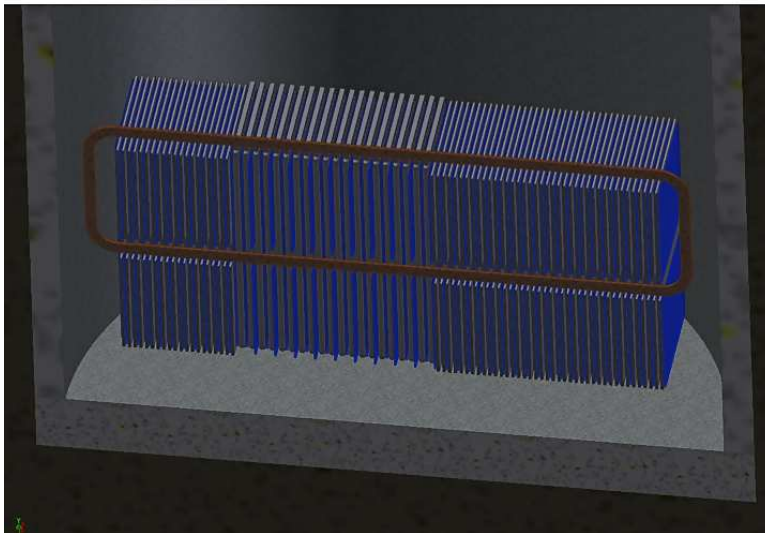


FIG. 10: A detector that could be employed in a shaft at the near site. The detector has a toroidal field and a central region with high-pressure gas argon targets.

and it measures the muon neutrino and anti-neutrino event rates as a function of (anti)neutrino energy before they are significantly altered by neutrino oscillations.

D. Reduced Cost Option: Placement of a Surface Detector in the LBNE Beamline

In neutrino mode, for the Homestake 10 kTon option, using $\delta_{CP} = 0^\circ$, the expected number of signal events for the normal mass hierarchy is ~ 200 and the expected number of background is ~ 80 events (see Appendix). In antineutrino mode, the corresponding number of signal events is ~ 60 and the number of background-events is 40. For $\delta_{CP} = -90^\circ$ ($+90^\circ$), the number of signal goes up (down) by ~ 40 events; the background remains unaltered. In the energy range, $0.5 \leq E_{\text{vis}} \leq 8$ GeV, the three sources, NC, ν_μ CC, and beam ν_e contribute equally to the background – the NC events contribute more at the lower energy end, while the CC events more above the first oscillation maximum. The statistical error of the (200+80) events is 16. Therefore, so long as the systematic error of the background (~ 80 events) remains much smaller than 16, the quality of the MH and CP violation sensitivities will not suffer. Therefore, the task for the ND in phase-I of LBNE is to measure the three backgrounds with a precision of $\sim 15\%$.

The ND must measure π^0 from NC and ν_μ CC interactions at $E_\nu \sim 2.5$ GeV. The least expensive, and the easiest option, is an LAr-ND on the Surface (LBNE-NDoS). One option is to put an existing LAr detector on the surface of the LBNE beamline; for example, the 35 ton detector under consideration could be placed atop the absorber-hall. Such an on-surface detector is operating in the NO ν A project (NO ν A-NDOS). Figure 11 shows the ν_μ spectrum originating from the NuMI beamline in the NO ν A-NDOS. The ν_μ from π^+ (blue-histogram) and K^+ (red-histogram) exhibit distinct Jacobean peaks. Figure 12 shows the corresponding ν_μ spectrum originating from the new LBNE beamline for the detector on the surface. The shapes of the ν_μ spectra in the NDoS are similar in the NuMI and LBNE beam-lines. Given the resolution of LAr detectors, it is clear that LBNE-NDoS will well measure π^0 production in the energy range 0.5–5 GeV. Furthermore, as Figure 12 shows that in a 35 ton LAr TPC, there will be ample statistics to measure π^0 production in the 2.5 GeV region where the first oscillation maximum occurs. It should

be noted that the MicroBooNE detector will measure the π^0 yield in ν -Ar interactions below 2 GeV.

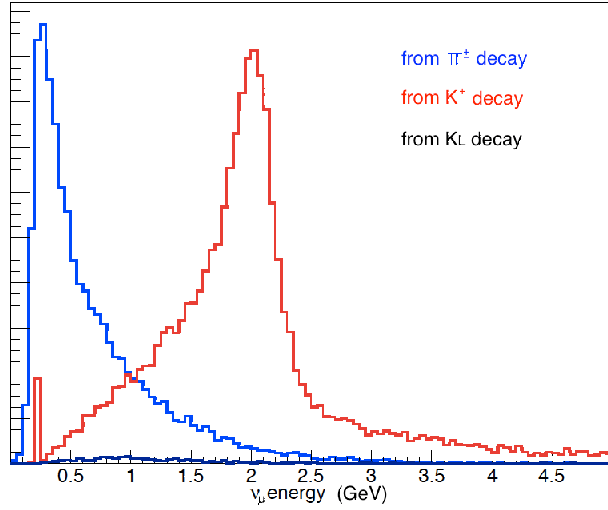


FIG. 11: The ν_μ spectrum in the NO ν A-NDOS. The ν_μ from K^\pm and π^\pm are shown in red and blue histograms. The small K_L contribution convey the level of ν_e expected in the NDoS.

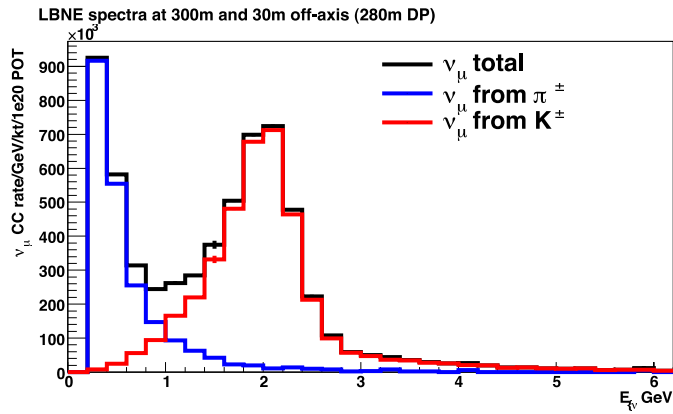


FIG. 12: The ν_μ spectrum, from the LBNE beamline, expected in a surface detector. The Jacobean peaks are rather similar to those expected in the NO ν A-NDOS. The figure also conveys that there will be ample statistics in a 35 ton LAr detector.

The LBNE-NDoS will be manifestly off-axis, exhibiting neutrino spectra different from that observed by the LBNE far-detector. for example, the NO ν A-NDOS cannot measure the NuMI neutrino-spectra in the FD in MINOS or NO ν A. Figure 13 shows the combined ν_μ and $\bar{\nu}_\mu$ spectra in the on-axis MINOS-ND before and after tuning the π^\pm/K^\pm production cross-sections to the observed neutrino data in the MINOS-ND. The spectra are different from the NDoS spectra because on- and off-Axis detectors sample different kinematic phase space (P_z versus P_T) of the π^\pm/K^\pm decays. The on-axis re-weighting for π^\pm and K^\pm in the P_z and P_T plots are shown in Figure 14, as gleaned from the MINOS-ND analysis. The NuMI-based detectors at the near site, however, (MINOS-ND, NO ν A-ND, and NO ν A-NDOS) provide us with a suite of measurements to project the on-axis flux in LBNE using the off-axis spectra. Additionally, at the NuMI near

site, the MicroBooNE detector (off-off-axis) will have been operational for several years providing further constraints. Finally, one has the charge-separation in the MINOS detectors, ND and FD, which calibrates the ν_μ vs $\bar{\nu}_\mu$ contamination in the neutrino beam created by 120 GeV protons.

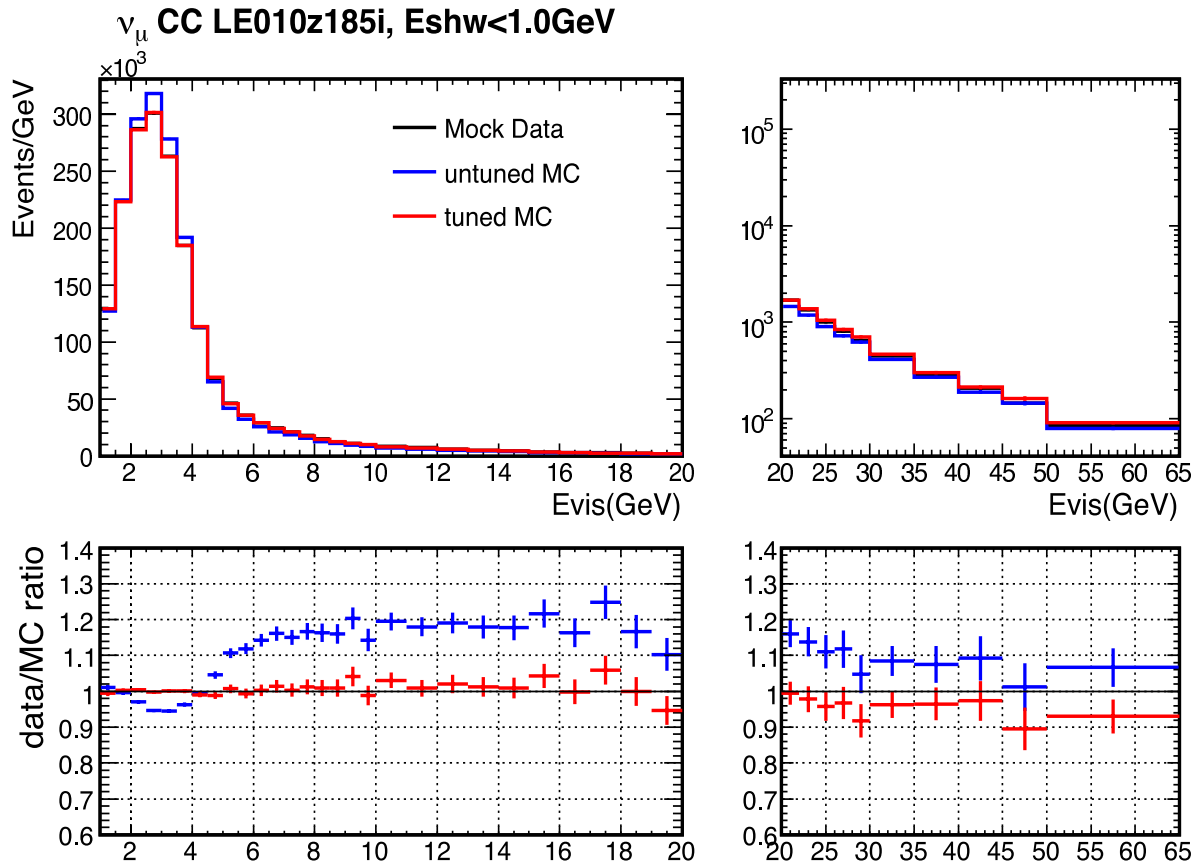


FIG. 13: The ν_μ and $\bar{\nu}_\mu$ spectra in the on-axis MINOS-ND in LE mode.

In summary for LBNE Phase-I, we could put an existing LAr detector (LAr-ND) on the surface – possibly the 35 ton detector under consideration, and possibly atop the absorber hall at the end of the LBNE decay-pipe. (A possible concern is the amount of beam-muon impinging the detector at this site.) Such an arrangement will provide the π^0 production in the NC and CC. The suite of NuMI near detectors — NO ν A-NDOS, NO ν A-ND, and MINOS-ND — in conjunction with the LBNE-NDoS will yield the on-axis LBNE neutrino and antineutrino spectra; and such a strategy will be inexpensive.

1. The ND Analysis Steps

In this section we outline a method for using a surface detector, for example above the absorber hall. It would be an existing LAr TPC detector — the 35 ton LAr detector under consideration — for the Phase-I of LBNE. The LBNE-NDoS will yield π^0 measurements in the 0.5–5 GeV neutrino energy region. The off-axis spectrum, however, will be drastically different from the on-axis spectrum expected at the FD. However, using the set of NuMI near-detectors — NO ν A-NDOS, NO ν A-ND, and MINOS-ND — an inexpensive and empirical path is laid forward to determine the backgrounds to $\pm 15\%$ precision for the MH and CP violation measurements. The salient analysis steps are:

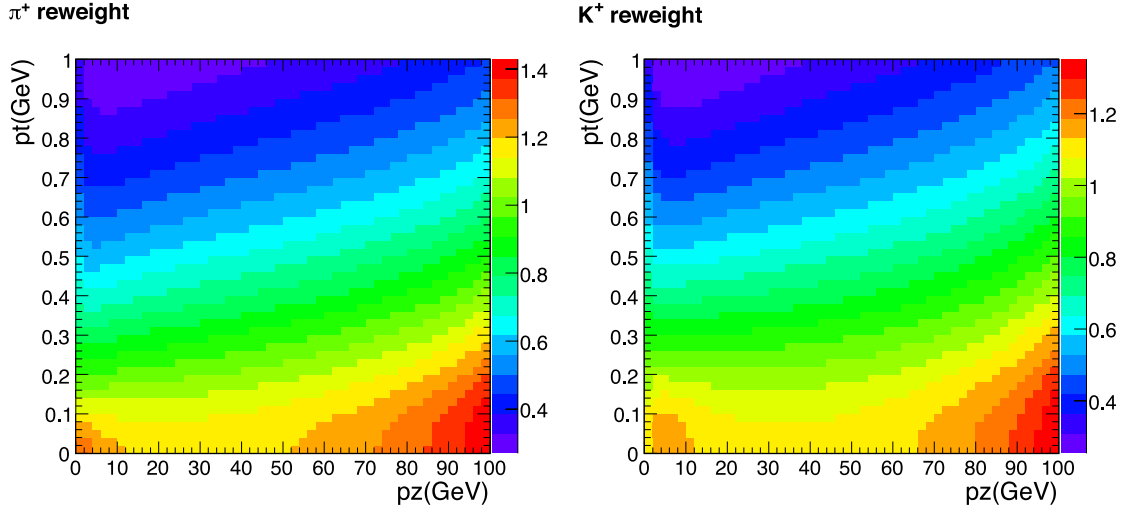


FIG. 14: π^+ and K^+ re-weighting as a function of linear and transverse momenta achieved in MINOS analysis.

1. Measure the neutrino spectra in NuMI-beam line using NO ν A-NDOS, MINOS-ND, and NO ν A-ND. The MicroBooNE data will provide additional constraint on the off-axis neutrinos and ν -Ar cross-sections below 2 GeV. Finally, the MINOS-FD and NO ν A-FD data will provide redundant checks on the neutrino spectra from π^\pm and K^\pm .
2. Understand and quantify the on-axis versus off-axis neutrino spectra based upon the set of measurements in (1). This involves π^+/K^+ and π^-/K^- induced spectra (P_z vs P_T) and constraining the K/π yield needed for the ν_e and $\bar{\nu}_e$ predictions.
3. Place the existing 35 ton LAr detector on the surface in the LBNE beamline. The station could be on/near the absorber hall, *i.e.* minimize expense on the conventional facility.
4. Measure the π^0 yield in NC and CC in the neutrino energy range 0.5–5 GeV in LBNE-NDoS. This takes care of the π^0 -induced backgrounds in the MH and CP violation analyses.
5. Using the NuMI data, steps (1) and (2), and the LBNE-NDoS obtain the on-axis spectrum in LBNE.
6. LBNE-NDoS will provide K/π , which in conjunction with (2) will yield a measure of ν_e and $\bar{\nu}_e$ in the beam.
7. LBNE-NDoS will measure the small ν_e and $\bar{\nu}_e$ contamination in the beam with better resolution than the NO ν A or MINOS detectors. These events, $\sim 0.6\%$ of the more abundant ν_μ will have a flat energy spectrum, similar to the K_L -induced ν_μ s as shown in the Figure. This measurement provides a redundant check of step (6).
8. Finally, control samples in the FD will yield additional constraints on the π^0 backgrounds and the flux (Section V A). The $\nu_2 \rightarrow \nu_3$ oscillations will have been very well measured, and these parameters in conjunction with the ν_μ and $\bar{\nu}_\mu$ CC data in FD will provide constraints on the background for the MH and CP violation measurements.

Although detail estimation must await full simulation, in our judgment the ND-strategy and the analysis outline presented above will adequately constrain the backgrounds for the phase-I Homestake option for LBNE.

VI. FUTURE PROSPECTS

In a new generation neutrino oscillation experiment, such as LBNE, the increased intensity of the beam and the increased scale of the FD will greatly enhance the number of events detected. On the other hand, the discoveries that we seek will be considerably more subtle than in MINOS or NOvA. In these circumstances, the systematic error, especially in regards to phenomena beyond the existing PMNS paradigm, will have to be precisely measured by a the ND complex, as envisioned in the full LBNE proposal, since the ability to constrain systematic error rests mainly on the competence of the ND and associated measurements and simulations.

In greater detail, the ND will fulfill four principal goals:

1. It will determine the absolute and relative abundances of the four neutrino species, ν_μ , $\bar{\nu}_\mu$, ν_e and $\bar{\nu}_e$ in the LBNE beam as a function of neutrino energy.
2. It will determine the absolute energy scale, a factor which determines the value of the Δm^2 parameter.
3. It will determine the rate of charged and neutral pion production both in NC and CC interactions. Pions are a predominant source of background in both the appearance and disappearance measurements.
4. It will determine neutrino cross sections on argon. Knowing the cross sections at the energies typical of the LBNE beam is essential for predicting both the signal and the background.

Such an LBNE ND complex will perhaps be the most precise neutrino apparatus for cross-sections, electroweak parameters, and new searches attracting contributions outside the DOE.

VII. CONCLUSIONS

Previously[1] it was argued that the US should pursue the best option for accelerator neutrino physics which is the longer baseline (1300 km) towards Homestake with a new optimized broadband beam. With the discovery of non-zero θ_{13} , the longer baseline towards Homestake offers the possibility of obtaining a statistically robust spectrum of muon and electron neutrinos and anti-neutrinos with large oscillation effects. Such a measurement is scientifically extremely well-motivated and well-appreciated as a unique capability in the U.S. by the international scientific community and by the funding agencies.

Under the guidelines of funding limitations for the first phase of the program the steering committee evaluated 1) the Homestake option with a surface far detector, 2) the NuMI option with a detector underground in the Soudan mine, 3) the NuMI option with a surface far detector near the NoVA site at Ash-River. The steering committee has clearly communicated the preference for the longer baseline to Homestake based on the detailed scientific evaluation by the physics working group and despite the difficult financial issues regarding the size and depth of the far detector as well as the scope of the near detector complex.

In this note, we have performed an initial assessment of the near detector scope. This assessment comes from a very experienced team of scientists who have performed many neutrino beam experiments in the past and have developed considerable judgment regarding the requirements on the near detector, associated instrumentation, and simulation software. For the full scope of LBNE in which detailed high statistics measurements of the electron neutrino and anti-neutrino appearance spectra are expected, a full scale near detector with similar performance and the same target nucleus as the far detector is needed. Indeed, one of the arguments in favor of a liquid argon TPC for the far detector (instead of a water Cherenkov detector) was the idea that a near-identical near detector could be utilized for a LAr TPC, whereas for a water Cherenkov detector an identical near detector is not possible. It is well known that such a near detector complex will

be very useful for a large number of subsidiary measurements that will enhance the productivity of the LBNE enterprise. We recognize, however, that in any of the Phase-I scenarios the financial constraints prevent the realization of the full scope unless we obtain non-DOE resources. Such efforts to obtain international contributions have started, but they require that we take the next steps for the approval of the LBNE project in the US.

In this note we have examined the statistical and systematic precision that we are expected to obtain in Phase-I. For the appearance analysis we have shown that the statistical precision will most likely be $\leq 10\%$ for the Homestake option. For the background, which is expected to be about 30% of the total rate, systematics need to be kept lower than $\sim 15\%$. The situation is more complex with the disappearance mode where the statistics are expected to be higher, but the signal is also very pronounced as an oscillatory shape on the spectrum. If the near detector requirements are defined narrowly for Phase-I to allow only an initial measurement of the mass hierarchy and CP violation, then our experience shows that there are various strategies for the near measurements that may not require the full scope of the near detector.

An examination of previous experience with experiments that did not have a near detector suggests that systematic errors of $\sim 10\%$ on the background could be reached. The confidence in the background estimate will be higher for a far detector that has much more detailed event reconstruction and particle identification. The choice of LAr TPC for the far detector in this case should serve us well.

Even in the reduced configuration, it would be valuable to have both a good measurement of muon and anti-muon neutrino spectra with a magnetic spectrometer as well as a measurement of neutral current events with π^0 's from the argon target nucleus for Phase-I. In this note we have suggested two solutions that might be feasible with considerably reduced costs. A magnetized near detector could be placed in a single shaft after it is commissioned on the surface. Secondly, an existing liquid argon TPC could be placed on the surface to detect off-axis neutrinos and measure the π^0 production rate. Both of these strategies could be coupled with previous measurements from the NuMI or MicroBoone experiments. A joint fit using all of these data would constrain the LBNE far detector backgrounds with adequate systematic error. These strategies will require close co-ordination and a common analysis framework for the neutrino beam experiments at Fermilab.

The defining characteristic for the Long-Baseline Neutrino Experiment is the length of the baseline. The preference from the FNAL steering committee will allow us to proceed with the longer baseline approach with comprehensive measurements of the 3-neutrino mixing model. We are confident that for Phase-I of LBNE a number of strategies are available with much reduced near detector scope to allow fundamental measurements of mass hierarchy and CP violation. Nevertheless, the near detector is very important for the ultimate success and precision of the LBNE program, and it is important to find appropriate resources to construct it in a timely way.

Appendix A: Appendix

1. ν_e Appearance Event Rate Tables

Expected signal and background event rates for the ν_e and $\bar{\nu}_e$ appearances measurements in the various LBNE reconfiguration options. The same assumptions about expected signal efficiencies and background rejection are used in each case [3].

configuration	signal	total bkg	ν_μ CC	NC	beam ν_e
Homestake 10 kton, NH	217	79	24	19	36
Soudan 15 kton, NH	375	419	159	81	180
Ash River 30 kton, NH	382	230	49	32	149
Homestake 10 kton, IH	95	79	24	19	36
Soudan 15 kton, IH	207	419	159	81	180
Ash River 30 kton, IH	217	230	49	32	149

TABLE III: *Expected event rates in neutrino mode for 5 years of neutrino running at 700 kW (6×10^{20} POT/year at 120 GeV) assuming $\sin^2 2\theta_{13} = 0.09$ and $\delta_{CP} = 0$. Rates are summed from 0.5 – 8 GeV.*

configuration	signal	total bkg	ν_μ CC	NC	beam ν_e
Homestake 10 kton, NH	62	43	12	13	18
Soudan 15 kton, NH	144	237	79	60	98
Ash River 30 kton, NH	130	142	28	21	94
Homestake 10 kton, IH	85	43	12	13	18
Soudan 15 kton, IH	118	237	79	60	98
Ash River 30 kton, IH	141	142	28	21	94

TABLE IV: *Expected event rates in antineutrino mode for 5 years of neutrino running at 700 kW (6×10^{20} POT/year at 120 GeV) assuming $\sin^2 2\theta_{13} = 0.09$ and $\delta_{CP} = 0$. Rates are summed from 0.5 – 8 GeV.*

2. ν_μ Disappearance Spectra

Figure 15 shows the expected signal and background rates for the ν_μ and $\bar{\nu}_\mu$ disappearance measurements in a 34 kton FD at the various baseline options. These rates have been scaled to the appropriate reconfiguration masses in Figure 6. The same assumptions about expected signal efficiencies and background rejection in LAr have been used in each case [3].

-
- [1] M. Diwan, LBNE public document, DOCDB-5962, <http://lbne2-docdb.fnal.gov:80800059005962004diwan-summary.pdf>
- [2] M. Diwan, LBNE internal document, docdb # 3648.
- [3] T. Akiri *et al.*, arXiv:1110.6249 [hep-ex].
- [4] A.K. Mann, editor, “Neutrino interactions with electrons and protons”, Key Papers in Physics series, AIP, 1993, ISBN-1-56396-228-4.

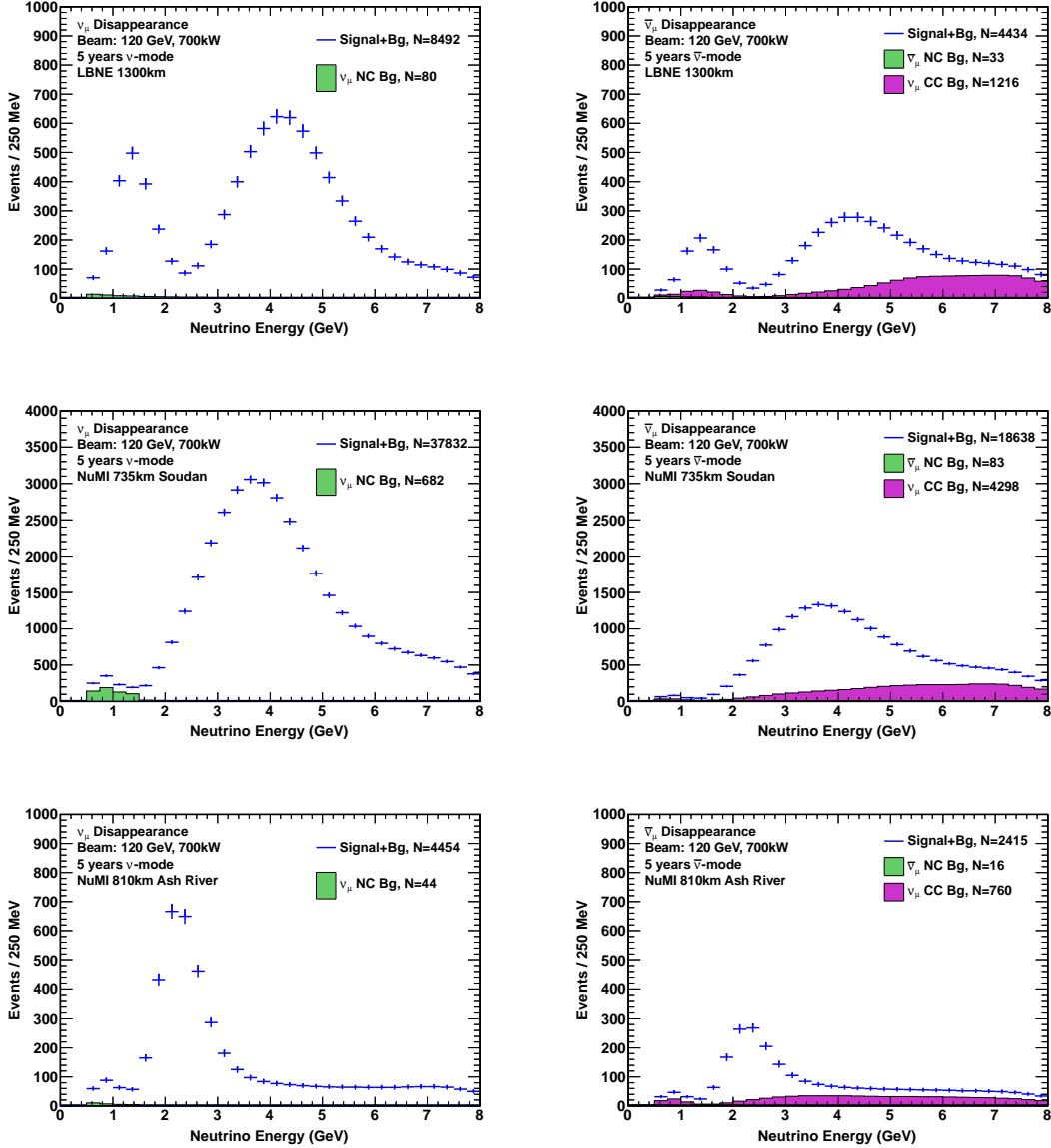


FIG. 15: *Expected spectra of oscillated ν_μ (left) and $\bar{\nu}_\mu$ (right) events for a 34 kton far detector at Homestake (top), Soudan (middle), and Ash River (bottom) assuming $\Delta m_{23}^2 = 2.3 \times 10^{-3} \text{ eV}^2$ and $\sin^2 2\theta_{23} = 0.705$. Listed event rates have been summed from 0-8 GeV. Plots are from Z. Ivan (BNL).*

- [5] B. Blumenfeld *et al.*, Phys. Rev. Lett. 62, 2237 (1989).
- [6] L. Borodovsky *et al.*, Phys. Rev. Lett. 68, 274 (1992).
- [7] S.R. Mishra, Prog. Part. Nucl. Phys. 64, 202 (2010).
- [8] A.A. Aguilar-Arevalo *et al.*, Phys. Rev. Lett. 105, 181801 (2010); Phys. Rev. Lett. 102, 101802 (2009).
- [9] A.A. Aguilar-Arevalo *et al.*, arXiv:1207.4809 [hep-ex].
- [10] G. Cheng *et al.*, Phys. Rev. D84, 012009 (2011).
- [11] K.B. Mahn *et al.*, Phys. Rev. D85, 032007 (2012); A.A. Aguilar-Arevalo *et al.*, Phys. Rev. Lett. 103, 061802 (2009).

- [12] P. Adamson *et al.*, Phys. Rev. Lett. 103, 261802 (2009).
- [13] P. Adamson *et al.*, Phys. Rev. D82, 051102 (2010).
- [14] P. Adamson *et al.*, Phys. Rev. Lett. 107, 181802 (2011).
- [15] R. Nichol. 'Results from MINOS,' Neutrino 2012, June 5, 2012.
- [16] T2K Letter of Intent: Neutrino Oscillation Experiment at JHF (2003), http://neutrino.kek.jp/jhfnu/loi/loi_JHFcor.pdf.
- [17] Y. Fukada *et al.*, Nucl. Instr. Meth. A501, 418 (2003).
- [18] J-PARC TDR, K2K-Report 2002-13 and JAERI-Tech 2003-044, <http://hadron.kek.jp/~accelerator/TDA/tdr2003/index2.html>.
- [19] T. Nakaya for the T2K Collaboration, "Results from T2K", the XXV International Conference on Neutrino Physics and Astrophysics, Kyoto, Japan, June 3–9, 2012, <http://neu2012.kek.jp/>.
- [20] S. Mine *et al.*, Phys. Rev. D77, 032003 (2008).
- [21] Laura Loiacono, MINOS, University of Texas Ph.D. thesis, 2011.